Liver And Hepatic Tumors Segmentation in 3-D CT Images

Christo Ananth[1], D.L.Roshni Bai[2], K.Renuka[3], A.Vidhya[4], C.Savithra[5]

Abstract— Medical imaging is an important technique for diagnosis and treatment planning today. A new proposed method of fully automatic processing frameworks is given based on graph-cut and Geodesic Graph cut algorithms. This paper addresses the problem of segmenting liver and tumor regions from the abdominal CT images. A predicate is defined for measuring the evidence for a boundary between two regions using Geodesic Graph-based representation of the image. The algorithm is applied to image segmentation using two different kinds of local neighborhoods in constructing the graph. Liver and hepatic tumor segmentation can be automatically processed by the Geodesic graph-cut based method. This system has concentrated on finding a fast and interactive segmentation method for liver and tumor segmentation. In the preprocessing stage, the CT image process is carried over with mean shift filter and statistical thresholding method for reducing processing area with improving detections rate. Second stage is liver segmentation; the liver region has been segmented using the algorithm of the proposed method. The next stage tumor segmentation also followed the same steps. Finally the liver and tumor regions are separately segmented from the computer tomography image.

Keywords— Automatic segmentation; graph-cuts; Geodesic Graph cuts; hepatic tumors and liver;

I. INTRODUCTION

Liver cancer is one of the most popular cancer diseases and causes a large amount of death every year. The liver cancer is one of the most common internal malignancies worldwide. Among the predominant cancer types, liver cancer ranks at fourth place and is a rising cause of death in the world. Each year, 1million new patients are diagnosed with primary liver cancer, of which approximately 60% died in 2002.

[1] Assistant Professor/ECE, Francis Xavier Engineering College, Tirunelveli

[2] U.G.Scholar/ECE, Francis Xavier Engineering College, Tirunelveli

[3] U.G.Scholar/ECE, Francis Xavier Engineering College, Tirunelveli

[4] U.G.Scholar/ECE, Francis Xavier Engineering College, Tirunelveli

[5] U.G.Scholar/ECE, Francis Xavier Engineering College, Tirunelveli

The development of these imaging technologies is the first step towards improvement of diagnosis accuracy and patient quality of life. Computed Tomography (CT) is probably the most widely adopted medical image technology build on X-rays transmission, that allows through image processing techniques to get 2-D cross-section images and then, from a stack of 2-D slices, a 3-D organ reconstruction.

Moreover, CT images, thanks to their high resolution, have been largely used for diagnosis of liver disease and volumetric measurements for medical operation, as in the case of resection or transplantation. Indeed, additional image analysis tools, as 3-D visualization of the patient liver, can help surgeons to plan suitable treatments. Surgical resection of hepatic tumors remains the first choice for curative treatment of primary and secondary liver malignancies. In this work, a new imaging approach and related algorithms for noninvasive diagnosis of liver tumors and subsequent monitoring of therapeutic treatments are presented. A fundamental point is represented by recent advances in image processing techniques, such as medical image segmentation. Indeed, the liver segmentation is an essential step for medical image analysis. In fact, it should be noticed how the segmentation results very often represent an input for 3-D navigation and display systems used for visualization, surgical planning, and radiation therapies.

Despite the multitude of automatic and semiautomatic literature- reported methods for liver segmentation, actual adoption of such approaches still presents several practical difficulties. This causes the usual employment in clinical routine of manual delineations of liver contours and tumors on diagnostic images, with consequent delineation enormous time and mental efforts for experienced doctors and operators, besides an intrinsic low reproducibility. For that reason, the development of efficient automatic methods is one of the most focused research topics: it can allow increasing radiologists' productivity, more objective and accurate diagnosis and more reproducible quantitative and quality result. In these perspectives, feasibility, in-depth analyses, and assessments of automatic segmentation accuracy and time performances are of paramount importance. To date, still the problem of tissue segmentation is to delimit the image areas representing different anatomies. This remains a challenging task due to the considerable overlap of soft tissues with strong intra-organ variation, to major human anatomical variations in liver

ISSN: 2278 – 1323

shapes and to similar voxel intensities of nearby organs. Furthermore, the detection of liver tumors is challenging because they are not clearly distinguishable from healthy tissues due do to the liver itself, being an organ with a high level of vascularization, automatic image processing have a high risk of wrong interpretation in terms of tissue segmentation. For clinical exploitability, the liver tumor segmentation must be able to cope with the variation in shape of tumors and with similar grey intensity of liver parenchyma.

The final output of segmentation in terms of knowledge regarding the exact spatial location and volume of segmented tumors is fundamental information for tumors medical treatments. In recent years, to overcome the inherent difficulties outlined above, computer-aided diagnosis (CAD) has been vigorously investigated to get more and more accurate liver segmentations. Such research investigations can be categorized into two main approaches: intensity-based and model-based methods. The former combine thresholding and morphological filtering normally resulting in robust approaches even if accurate segmentations need the setting of several parameters depending on processing step, modality, etc. Instead, model-based approaches are currently the main research track, generally based on active contours with level sets or snake, statistical model are also reported. Mahr *et al* reviewed and compared the various techniques which included region-growing, isocontour, snakes, hierarchical and histogram-based methods, and found that region-growing and snakes (i.e., active contour models), were the most promising for future investigation on liver volumetry determination. In addition, Boykov and Kolmogorov showed the feasibility of liver segmentation by means of graph-cut technique on the liver case. However, all these methods require a manual initialization based on learning database or on user interfaces introducing limitations mainly related to subjectivity and human errors.

In this work, in order to get liver and liver tumors segmentations totally independent from operator's intervention from contrast enhanced CT volume images, a 3-D initialization method was developed and its reliability was tested through graph-cut and Geodesic Graph Cut techniques. In the previous work, a new method is described for fast segmentation of liver using Graph cut algorithm from CT volume images. In that work, two different approaches were used for segmentation of liver volume and for related tumors. In this new study, the same segmentation method is applied for liver and for its internal pathological structures. Therefore, the initialization method is further developed making it suitable also for the Geodesic graph cut algorithm. The aims of this comparative evaluation were: 1) verify the feasibility of two different segmentation approaches and their automation starting from the same adaptive initialization method; 2) apply both segmentation approaches to the liver and to the hepatic tumors employing twice exactly the same initialization method for liver and then for tumor initialization; and 3) comparatively assess the segmentation results concerning liver volumes and tumors with respect to radiologist manual segmentation taken as the ground truth.

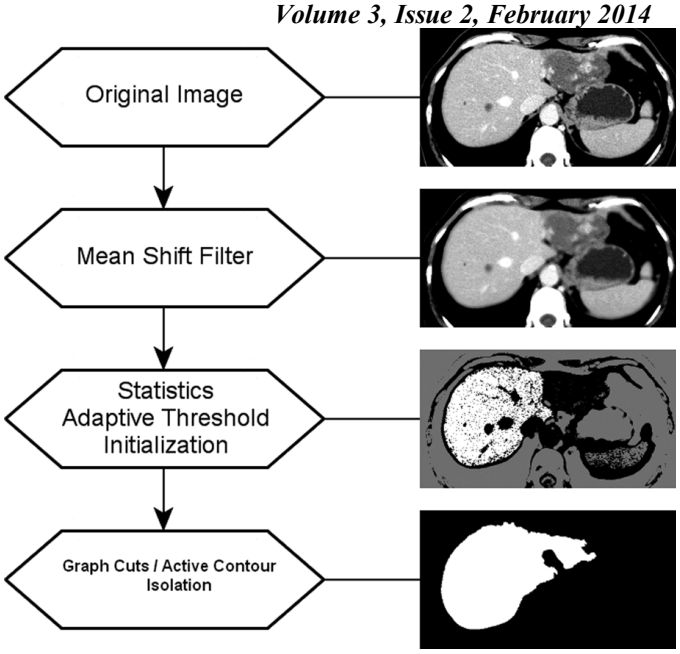

Figure l. Flowchart of the automatic liver initialization method.

In this study, datasets of different patients were processed using the above automatic mentioned method and the results were compared with respect to manual segmentation carried out by an expert radiologist, that is considered the available reference standard.

II. MATERIALS AND METHODS

For any liver local treatments, it is necessary to identify and localize the liver surface, the tumors, the topography of blood vessel, and the spatial relationship between tumors and structures. To meet these challenges various algorithms have been developed using pixel-based or/and contour-based methods. Currently, two approaches are under investigation. The first one is Geodesic Graph cut approach and the second method is the graph cuts that is one of the current cutting edge technique in image segmentation.

A. Automatic Liver Initialization Method

Model-based segmentation methods usually require a preliminary initialization by operators prior to their application. In this specific case, active contours needs, as an input, a first course outline of the liver while graph-cuts need samples of both liver and background labels. Here, an automatic initialization method is applied to both techniques (Fig. 1). This method is based on a statistical model distribution of liver average intensity and its standard deviation. Before applying the statistical distribution model, in order to obtain the initialization data input, preliminary preprocessing steps are required as following detailed. First of all, a preprocessing filter needs to be applied to the original volumetric image for noise removal from homogenous areas while keeping clear and sharp edges. The best results were obtained with the mean shift filter most suitable for these purposes. Second, considering the resolution of the processed images, each slice of the filtered volume was divided into 64 squared sub regions, presenting in this way enough pixels for estimations and statistical relevance of regional calculations. Then, for each abdominal

ISSN: 2278 – 1323

sub region, the mean image intensity and its standard deviation were calculated to identify the most homogeneous regions in terms of pixel intensity (i.e., regions with standard deviation lower than 1% of the peak value of corresponding histogram).

Among these latter, the median was selected to be representative of liver regions with corresponding standard deviation. So, as illustrated above, implementing our adaptive threshold technique on this automatically extracted patient- specific data, the images were partitioned and then liver regions identified. Finally, these identified regions were further and more accurately segmented [Fig. 2(b) and (c)], through Graph cut and Geodesic graph-cut approaches as described in the following sections.

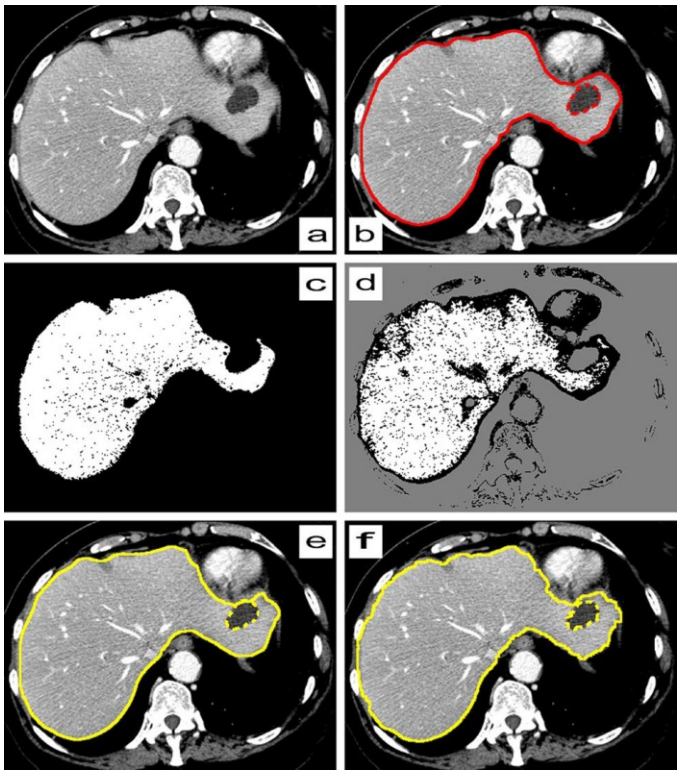

Fig. 2. (a) Original image. (b) Manual segmentation made by an expert radiologist. (c) Liver surface initialization for active contour. (d) Liver surface initialization for graph-cut (in white: liver, in gray: background and in black: undetermined voxels). (e) Graph cut segmentation. (f) Geodesic Graph-cut segmentation (the plain line represents the liver surface, while the dashed line represents the tumor contour).

B. Automatic Tumor Initialization Method

This step was applied only to liver volume, obtained after automatic delineation of liver surface: this latter, applied to original dataset volume, was used as a mask in order to prevent processing overloads and avoid errors related to the presence of surrounding tissues presenting similar gray scale distributions. Additionally, for this purpose, the voxels belonging to the intensity range domain were also removed from the segmented liver volume. This intensity range domain is selected because the data fitted to Gaussian distribution and nearly all (99.7%) of the values lied within three standard deviations of the mean. This choice allowed the correct identification of liver respect to other organs, optimizing the calculation resources and increasing the tumor segmentation accuracy. The histograms of the anatomical structures of liver are showed in Fig. 3.

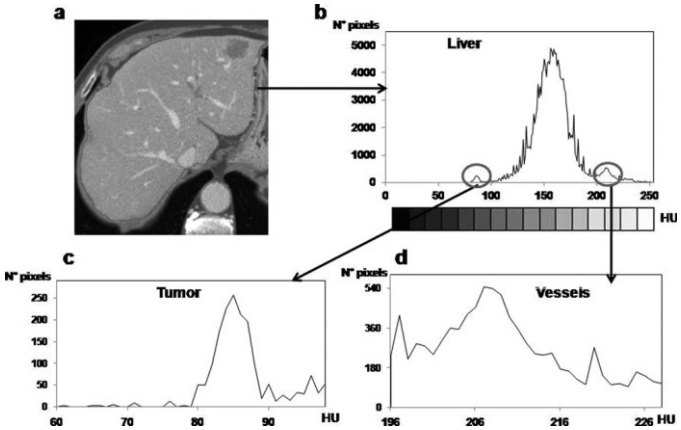

Fig. 3. Gray-level histograms related to structural components of: (a) segmented liver, (b) histogram of whole liver, (c) zooming of histogram related to tumors, and (d) zooming of histogram related to vessels.

In conclusion, the Gaussian distribution with lowest Hounsfield units (HU) values corresponds to tumor intensities, and then the average tumor intensity value and its standard deviation were extracted from the histogram thanks to a cross-correlation with a Gaussian shaped function. These were used to identify tumor voxels in the partitioned liver regions that represented the input for the final segmentation step.

C. Patient Datasets

The used CT volume datasets reflect indeed an average quality of the technology and competence and should present a more general meaning in term of final applicability and effectiveness. The only limitation for data selection was related to the image resolution needed for a coherent final result assessment. Then, imaging CT protocols followed the clinical routine in use in each hospital for imaging abdominal cancers with portal vein phase contrast enhancement. Moreover, accordingly with the aim of this paper, final clinical therapies to patients were not influenced by the result of this work. In summary, 25 anonymized CT datasets from corresponding different patients were collected and retrospectively processed by means of previously mentioned algorithms. Image datasets were acquired on six different CT scanners (LightSpeed VCT, HiSpeed NX/I, LightSpeed Pro 16, LightSpeed Plus – General Electric, Emotion 16 – Siemens, Brilliance 16 – Philips). Scanning acquisition parameters were the following: 120–130 kV voltage 250–375 mAs X-ray tube current and an exposure time between 700 and 1070 ms.

D. Geodesic Segmentation of Liver and Tumors

In cases where the color models inferred from the user's strokes are indistinct, geodesic segmentation can be improved by the inclusion of explicit edge information to encourage placement of selection boundaries on edges in the image and allow the user more freedom in placing strokes. In cases where the color models are more distinct, though, the

ISSN: 2278 – 1323

edge information (with inherent shrinking bias) is not as necessary. The region term alone can often carry the segmentation in such cases, but global color models without spatial locality information can often select disjoint regions. The use of geodesic distance rather than simple color-similarity alone can avoid this. This section presents how geodesic distances and edge information can be combined in a graph cut optimization framework, and then presents a way to use the predicted classification accuracy from the inferred color models to automatically tune the tradeoff between the strengths and weaknesses of the two.
The unary region term can be computed as follows:

$$R_l(x_i) = s_l(x_i) + M_l(x_i) + G_l(x_i) \quad (1)$$

where Ml(xi) is based on a global color model as is often used for graph-cut segmentation, Gl(xi) is based on geodesic distance, and

$$s_l(x_i) = \begin{cases} \infty & \text{if } x_i \in \Omega_{\bar{l}} \\ 0 & \text{otherwise} \end{cases} \quad (2)$$

indicates the presence of a user stroke where $\bar{l}$ is the label opposite l (i.e. if l = F, then $\bar{l}$ = B). We use the Fast Gauss Transform to compute the foreground/background color models Pl(c) for both global similarity and geodesic distances. $M_l(xi)$ is computed by

$$M_l(x_i) = P_{\bar{l}}(C(x_i)). \quad (3)$$

$G_l(xi)$ is computed by normalizing the relative foreground/ background geodesic distances

$$G_l(x_i) = \frac{D_l(x_i)}{D_{\mathcal{F}}(x_i) + D_{\mathcal{B}}(x_i)}. \quad (4)$$

For the boundary term we use:

$$B(x_i, x_j) = \frac{1}{1 + ||C(x_i) - C(x_j)||^2} \quad (5)$$

where C(x) Є [0,255].
To allow for global weighting of the relative importance of the region and boundary components,

$$E(\mathcal{L}) = \lambda_R \sum_{x_i \in P} R_{\mathcal{L}_i}(x_i) + \lambda_B \sum_{(x_i,x_j)\in N} B(x_i, x_j)\ |\mathcal{L}_i - \mathcal{L}_j| \quad (6)$$

Although separate region (λ_R) and boundary (λ_B) weights could be folded into a single weight, we choose to keep them separate to make their respective purposes clearer. The boundary weight serves the role of the traditional fixed region/boundary weighting in graph cut methods, and we adjust it to individual images by considering only the size of the image (due to the disproportionate scaling of an object's area (unary term) and perimeter (boundary term)). The region weight λ_R is the relative weighting of the geodesic distance and other region components. While the user could tune λ_R manually, this would require excessive tweaking and is undesireable; instead, we want to automatically tune this parameter on a per-image basis by predicting the segmentation performance of the geodesic distance term. To do this, the posterior probability of a pixel with color c belonging to foreground (F) or background (B) respectively is considered, assuming equal priors. As such, it is essentially functioning as a simple Bayesian classifier, the error in which can be estimated by

$$\varepsilon = \frac{1}{2}\left[\frac{\sum_{x\in\mathcal{F}} P_{\mathcal{B}}(C(x))}{|\Omega_{\mathcal{F}}|} + \frac{\sum_{x\in\mathcal{B}} P_{\mathcal{F}}(C(x))}{|\Omega_{\mathcal{B}}|}\right] \quad (7)$$

When there is no error (ε = 0), we would like to give the Color-based terms (M and G) full weight, and when the color models become indistinct (ε ≥0.5), we want to give them no weight:

$$\lambda_R = \begin{cases} 1 - 2\varepsilon & \text{if } \varepsilon < 0.5 \\ 0 & \text{otherwise.} \end{cases} \quad (8)$$

The geodesic and boundary terms are further weighted based on the local confidence u(x) of the geodesic components:

$$u(x_i) = \left|\frac{D_{\mathcal{F}}(x_i) - D_{\mathcal{B}}(x_i)}{D_{\mathcal{F}}(x_i) + D_{\mathcal{B}}(x_i)}\right|^{\gamma} \quad (9)$$

where empirically γ= 2 to 2.5 works well.
We redefine the region terms to weight the geodesic component by u(xi):

$$R_l(x_i) = s_l(x_i) + M_l(x_i) + u(x_i)G_l(x_i) \quad (10)$$

This maintains the weight of the geodesic distance term when relatively certain that the pixel xi is clearly in the objects interior or exterior (u(xi) close to 1) and decreases it near where geodesic segmentation would place boundaries (u(xi) close to 0). We also correspondingly spatially adapt the weighting of the boundary costs based on u(x) as follows:

$$B(x_i, x_j) = \frac{1 + (u(x_i) + u(x_j))/2}{1 + ||C(x_i) - C(x_j)||^2} \quad (11)$$

Note that when the average geodesic certainty of the two pixels is high, this suggests an object interior/exterior, and the cost of placing a cut here is further increased. When this geodesic confidence is low, this suggests that geodesic segmentation alone would consider this to be near a boundary, and we reduce the effect of the geodesic component, shifting control to the more accurate edge-finding term. The net effect of this spatially adaptive weighting is to both increase the relative weighting of the unary geodesic distance term and increase the cost of a boundary cut in what are clearly interior/exterior regions, while both decreasing the relative weighting of the unary geodesic term and decreasing the cost of a boundary cut in areas where we want to more accurately localize the object boundary.

E. Graph-Cut Segmentation Algorithm of Liver and Tumors

To discriminate liver from background, we set a range threshold equal to 2σ. The initialization rules are as follows:
1) v (voxel) Є liver, if I(v) (image intensity of voxel) Є L2 (liver domain) and v Є BIG
2) v Є Background if I(v) Є B2 (Background domain) or if I(v) Є L2 and v does not belong to BIG (biggest 18 connected component after thresholding)
3) v Є undetermined otherwise.

ISSN: 2278 – 1323

Here, Energy function relies on Region term and Boundary term. I (v) stands for the image intensity of voxel, and *BIG* for the biggest 18-connected component after similar thresholding. 3-D graph-cut method, conversely to active contour technique, is not iterative and is based on global minimization of defined energy function classes on a discrete graph. Energy function and penalties definitions were adapted to the specific liver segmentation purpose.

Then, energy function relies on two main terms: a) a region term (penalties depending on neighborhood context and on voxel labeling) and b) a boundary term (penalties based on adjacent voxels dissimilarity). For region term weights R_p, a patient-specific Gaussian model was used for the liver, thus providing a more faithful result than *a-posteriori* probability of object-labeled voxels. Then, for background, the *a-posteriori* probability was adapted taken into account all voxels but the ones initialized as liver in order to provide a non-null R_p also to undetermined voxels during initialization.

$$R_p(\text{obj}) = \exp \frac{\left(-\frac{(I_p-\mu_{\text{liver}})^2}{2\sigma_{\text{liver}}{}^2}\right)}{\sigma_{\text{liver}}\sqrt{2\pi}} \tag{12}$$

$$R_p(\text{bkg}) = -\ln \Pr(I_p \,\overline{obj}). \tag{13}$$

a-posteriori probability for R_p (bkg) was evaluated on the histogram of the mean-shift filtered image for the voxels that were not initialized as liver. For boundary term, "directed" edge weights $w_{p,q}$ seem the best solution to encourage cuts from brighter object to darker background like liver in CT scans, and were defined as follows:

$$w_{p,q} = \begin{cases} 1, & \text{if } I_p \le I_q \\ \exp\left(-\frac{(I_p-I_q)^2}{2\sigma^2}\right), & \text{if } I_p > I_q \end{cases}. \tag{14}$$

Here σ, enabled to adjust the range of intensities taken into account to find the edges. Indeed small σ^2 encouraged edges between voxels with about the same intensities, while for big σ^2, intensity range was wider enabling contours to evolve with less constraints.

The cost function E can be defined as follows:

$$E = \sum_{p,q} w_{p,q} \cdot \delta_{Sp \neq Sq} + \lambda \sum_{p} R_p(S_p) \tag{15}$$

where S_p and S_q can take the label values {liver or background} in order to find the minimum of E and the corresponding optimal set of segmentation S_p of all voxels .Cost function E and edge weights $w_{p,q}$ were used for the second run of the graph-cut technique, while the region term weights R_p were redefined as follows:

$$R_p(\text{tumor}) = \exp \frac{\left(-\frac{(I_p-\mu_{\text{tumor}})^2}{2\sigma_{\text{tumor}}{}^2}\right)}{\sigma_{\text{tumor}}\sqrt{2\pi}} \tag{16}$$

$$R_p(\text{tumor}) = \exp \frac{\left(-\frac{(I_p-\mu_{\text{tumor}})^2}{2\sigma_{\text{tumor}}{}^2}\right)}{\sigma_{\text{tumor}}\sqrt{2\pi}} \tag{17}$$

III. RESULTS

The automatic segmentation of liver surface and hepatic tumor was executed successfully for all patient datasets with both automatic segmentation techniques; Automatic liver segmentation by the Geodesic graph-cut algorithm succeeds to include these tumors (underneath the surface) inside the liver segmentation. The reason is that the Geodesic graph-cuts include neighboring contextual information enabling to overstep edges between tumors or vessel and liver parenchyma.

A. Liver Segmentation Accuracy

Both automatic techniques provided highly accurate liver surface segmentation with respect to the manual segmentation defined as the gold standard. Indeed, both algorithms reached quite similar good values for all comparative metrics defined in Table I. Geodesic Graph Cut algorithms and graph-cut algorithms produced a liver volume with a high level of overlapping given by an average DSC of 96.17% ± 0.87 and of 95.49 ± 0.66, respectively. Geodesic Graph Cut algorithm reached therefore a slightly better average DSC, but on nine cases over 25 (36%) Geodesic Graph Cut algorithm produced a liver surface segmentation with a higher DSC than graph cuts. FPR and FNR misclassification ratios were balanced with contemporary low values for both automatic approaches. The algorithm based on GVF active contours generated fairly equal false alarm rate (FPR = 3.87% ± 0.98) and undetection rate (FNR = 3.87± 0.98). In addition, over the set of 25 cases, the average Distance – Error was equal to 2.38mm ±0.41for Graph Cut method, while it was fairly better for Geodesic Graph Cut method with a value of 2.19 mm ± 0.59. Furthermore, for all these three metrics the paired -test provided a great result statistically significant with a 95% confidence interval.

TABLE I
COMPARISON OF LIVER SURFACE SEGMENTATION

Performance parameters	GRAPH CUT		GEODESIC GRAPH-CUT	
	Mean	Standard Deviation	Mean	Standard Deviation
DSC	96.16%	0.87%	95.49%	0.66%
FNR	3.87%	0.98%	5.10%	1.65%
FPR	3.35%	1.19%	2.35%	0.91%
DISTANCE ERROR	2.38 mm	0.41 mm	2.19 mm	0.59 mm

ISSN: 2278 – 1323

B. Tumor Segmentation Accuracy

Among the 52 hepatic tumors diagnosed in 25 patients, Geodesic graph-cut algorithm detected 48 tumors leading to a detection rate of 92.31%, while Graph cut algorithm detected 44 tumors for a detection rate of 84.62%. The differences between results produced by the two automatic algorithms were emphasized by three metrics as indicated in Table II. Regarding the volume overlapping of hepatic tumors, Geodesic graph-cut algorithm provided an average DSC of 88.65% ± 3.01, while Graph cut method reached a lower average DSC equal to 87.10% ± 2.99. In terms of misclassification, graph-cut algorithm presented again a lower average FPR than Geodesic algorithm (6.10% ± 2.52 versus 8.99% ± 3.95). However, the undetection rate was in favor of graph cut algorithm since its average FNR reached the value of 8.97% ± 2.26, while geodesic graph-cuts obtained an average FNR of 9.89% ± 2.93. Again, for all these three metrics the paired T–test provided a great result statistically significant with a least 90% confidence interval.

TABLE II
COMPARISON OF TUMOR SEGMENTATION

Performance parameters	GRAPH-CUT		GEODESIC GRAPH-CUT	
	Mean	Standard Deviation	Mean	Standard Deviation
DSC	87.1 %	2.99 %	88.65 %	3.01 %
FNR	8.97 %	2.26 %	9.89 %	2.93 %
FPR	8.99 %	3.95 %	6.10 %	2.52 %

Table III shows the average times required to obtain liver surface and hepatic tumor segmentations for both automatic methods. Both algorithms were run on a personal computer with 3.4 GHz CPU speed and 1 Gbyte of random-access memory. The indicated values are the average time needed for a single slice; these ones are normalized on the number of slices for each specific processed dataset. The Geodesic graph-cut algorithm always produced faster segmentation than Graph cut algorithm with an average processing time per slice equal to 10.9 s ± 1.1 and 11.5 s ± 1.1, respectively. Into these time values, mean shift filtering operation is included and represents most part of the required time, since it is equal to an average of 7.3 s ± 1.1 (Table III). Other preprocessing filters (convolution, median, or average filter, etc.) were assessed but segmentation results were not acceptable in view of the objective of this study: fully automatic process, accurate liver, and tumors extractions.

TABLE III
PROCESSING TIME

Processing Steps	GRAPH-CUT		GEODESIC GRAPH-CUT	
	Mean	Standard Deviation	Mean	Standard Deviation
Mean Shift Filter	7.310	1.014	7.310	1.014
Initialization	0.861	0.046	0.699	0.023
Liver Segmentation	1.505	0.196	1.009	0.096
Tumor Segmentation	1.796	0.128	1.945	0.308
Total	11.47	1.084	10.963	1.146

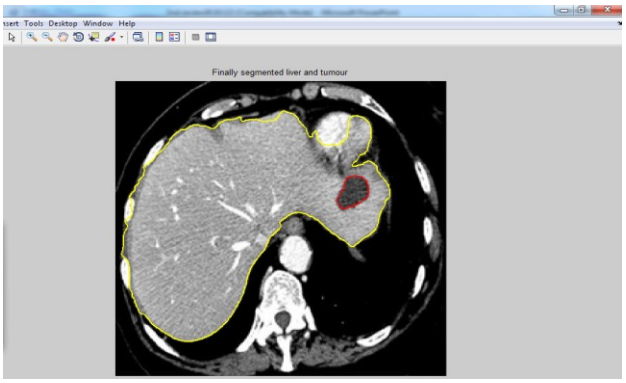

Fig. 4. Finally Segmented Liver and Tumor

IV. DISCUSSION

Adaptive initialization method allows a fully automatic liver and tumors segmentation employing Geodesic Graph cut or graph-cut based techniques. In the previous work, the initialization technique was applied to Graph cut algorithm demonstrating the robustness and effectiveness of automatic liver segmentation. In this study, the initialization method was further extended to Geodesic graph cut algorithm in order to enable full automation of this method and evaluate potential improvements with respect to previous automatic presented approaches and then to the ground truth. The same segmentation approaches were then applied also to segmentation of liver tumors. All segmentation results have been comparatively presented.

The evaluation framework used in this paper indicates that accurate results are reached by both approaches, as well for big objects like liver as for smaller ones like tumors. Even if the results are quite similar for liver surface segmentation, the Geodesic graph-cut algorithm takes its advantage over the Graph cuts algorithm in the number of tumors detected and in the fairly better accuracy of tumor segmentation. Indeed, it recognizes four tumors more, among the 52 diagnosed in study datasets. Therefore, the advantage of the Geodesic graph-cut technique over the Graph Cut method with their general approach in computer vision, is confirmed by this study for the specific problem of liver and hepatic tumor segmentation.

Moreover, the Geodesic graph-cut algorithm produces also better segmentation results than other fully automatic methods found in literature in both terms of accuracy and time processing. Lamecker *et al.* achieved also an accuracy of 2 mm but a preliminary 40 training datasets was required, while the latter obtained an accuracy of 1.5 mm but on a

ISSN: 2278 – 1323

rather small sample of five scans only. Initialization techniques had a fairly important impact on segmentation performance, but mainly regarding the computation time. Indeed, Graph cuts method are capable to evolve towards the real edges starting from a relatively far coarse segmentation thanks to the use of Graph cuts method.

The Geodesic graph-cut technique is also able to deal with lots of initially undetermined voxels. In addition, concerning the Geodesic graph-cut algorithm, any misclassification during the initialization process should be prevented in order to have proper region term weights for the background. Therefore, liver domains and were set to obtain optimal results for both methods. In comparison with the average 78 s/slice needed for manual liver segmentation, the processing time (10.9 s/slice in Table III) reached by the implemented automatic version of Geodesic graph-cuts presented in this work demonstrates the important potential time saving for this operation. In addition, the implemented Geodesic graph-cut technique produces accurate segmentation results always faster than the implemented Graph cut algorithm. Nevertheless, direct comparison of time performances available in literature is often difficult to be carried out since this consideration is rarely clearly reported and the execution environment is always different in terms of computational power. However, Automatic segmentation technique of liver region based on extracted blood vessels reported a processing time of 24 s/slice for automatic liver surface segmentation, while the method of Automatic liver segmentation for volume measurement in CT images required 1 min/slice for the same result. A processing time of about 5 min to obtain the all liver surface was reported but using semiautomatic methods.

Although the proposed study demonstrates the accuracy of both segmentation processes and improvements brought by Geodesic graph cuts with respect to Graph cuts, the primary limitation is that both methods encounter some difficulties to detect large hepatic tumors of the liver outer rim. These tumors are excluded from the liver surface volume and cannot be detected during the following step, since the liver surface segmentation is used as a mask to prevent false alarms. Indeed, even small tumors (0.9 cm) in the liver outer rim were undetected by Graph cuts method. However, this study demonstrates that Geodesic graph-cuts tend to overcome this limitation if tumor volume is reasonably not too big in size: tumor exclusion happened only when size exceeded 2.5 cm, which is a size usually easily detectable by a visual inspection.

Moreover, the accuracy of tumor segmentation is not as high as for liver surface, since tumors are generally smaller objects. So, an error of a constant voxel number is not proportionally worst in this case than for liver volume. Finally, it should be noticed how the prefiltering represents more than 70% of the total processing time, but this step is essential for accurate segmentations. Alternative filtering could be used in order to reduce time resources needed but reliability of the algorithm would suffer of this change.

V. CONCLUSION

In conclusion, this study presented the implementation of two fully automatic liver and tumors segmentation techniques and their comparative assessment. The described adaptive initialization method enabled fully automatic liver surface segmentation with both Graph cut technique and Geodesic graph-cut techniques, demonstrating the feasibility of two different approaches. The comparative assessment showed that the Geodesic graph-cut method provided superior results in terms of accuracy and did not present the described main limitations related to the Graph cuts method. The proposed image processing method will improve computerized CT-based 3-D visualizations enabling noninvasive diagnosis of hepatic tumors. The described imaging approach might be valuable also for monitoring of postoperative outcomes through CT-volumetric assessments. Processing time is an important feature for any computer-aided diagnosis system, especially in the intra-operative phase.

VI. FUTURE WORK

Future focus will be given towards time reduction needed for the image prefiltering also by employing more powerful computers. In addition, the satisfactory results obtained in tumor delineations may be exploited for future improvement regarding the detection of cysts.

REFERENCES

[1] World Health Organization (WHO), "European health report" Jan. 01,2002, vol. 97, European Series. [Online]. Available:http://www.euro.who.int/__data/assets/pdf_file/0007/98296/E76907.pdf

[2] K. M. Horton, D. A. Bluemke, R. H. Hruban, P. Soyer, and E. K.Fishman, "CT and MR imaging of benign hepatic and biliary tumors,"*Radiographics*, vol. 19, pp. 431–451, Mar.-Apr. 1999.

[3] S. J. Lim, Y. Y. Jeong, and Y. S. Ho, "Automatic liver segmentation for volume measurement in CT images," *J Vis. Commun. Image Represent.*,vol. 17, pp. 860–875, Aug. 2006.

[4] P. Lamata1, F. Lamata, V. Sojar, P. Makowski, L. Massoptier, S. Casciaro,W. Ali, T. Stüdeli, J. Declerck, O. J. Elle, and B. Edwin, "Use of the resection map system as guidance during hepatectom," *Surgical Endoscopy,* , no. ISSN 0930-2794, 1432-2218 –Cat. New Technology DOI 10.1007/s00464-010-0915-3, Feb. 2010.

[5] H. P. Meinzer, P. Schemmer, M. Schobinger, M. Noldena, T.Heimanna, B. Yalcina, G. M. Richterc, T. Krausb, M. W. Büchlerb,and M. Thorna, "Computer-based surgery planning for living liver donation," *Int Arch. Photogram Rem. Sens. Spatial Inform. Sci.*, vol.35, pp. 291–295, Jul. 2004.

[6] D. Verellen, M. De Ridder, and G. Storme, "A (short) history of imageguided radiotherapy," *Radiother. Oncol.*, vol. 86, pp. 4–13, Jan. 2008.

[7] Bai.X. and Sapiro.G. " A geodesic framework for fast interactive image and video segmentation and matting. IEEE ICCV 2007, pages 1–8, Jan 2007

[8] I. Ben-Dan and E. Shenhav, "Liver Tumor segmentation in CT images using probabilistic methods," in *Proc. 11th Int. Conf. Med. Image Comput. Comput. Assisted Intervention, MICCAI'08,*, New York, 2008, pp. 1–11.

ISSN: 2278 – 1323

[9] A. Mahr, S. Levegrün, M. L. Bahner, J. Kress, J. Zuna, and W. Schlegel, "Usability of semiautomatic segmentation algorithm for tumor volume determination," *Invest. Radiol.*, vol. 34, pp. 143–150, 1999.
[10] N. H. Abdel-massieh, M. M. Hadhoud, and K. A. Moustafa, "A fully automatic and efficient technique for liver segmentation from abdominal CT images," in *Proc. 7th Int. Conf. Inform. Syst. (INFOS)*, 2010, pp. 1–8.
[11] T. Saitoh, Y. Tamura, and T. Kaneko, "Automatic segmentation of liver region based on extracted blood vessels," *Syst. Comput. Jpn.*, vol. 35,pp. 633–641, May 2004.
[12] L. Soler, H. Delingette, G. Malandain, J. Montagnat, N. Ayache, C. Koehl, O. Dourthe, B. Malassagne, M. Smith, D. Mutter, and J. Marescaux, "Fully automatic anatomical, pathological, and functional segmentation from CT scans for hepatic surgery," *Comput.-Aided Surg.*, vol. 6, pp. 131–142, 2001.
[13] H. Jiang and Q. Cheng, "Automatic 3D segmentation of CT images based on active contour models," in *Proc. 11th IEEE Int. Conf. Comput.Aided Design and Graphics, CAD/GRAPHICS'09*, 2009, pp. 540–543.
[14] S. Pan and B. M. Dawant, "Automatic 3D segmentation of the liver from abdominal CT images: A level-set approach," in *Proc. SPIE Med.Imaging*, 2001, vol. 4332, pp. 128–138.
[15] J. Gao, A. Kosaka, and A. Kak, "A deformable model for automatic CT liver extraction," *Acad. Radiol.*, vol. 12, pp. 1178–1189, Sep. 2005.
[16] H. Lamecker, T. Lange, and M. Seebass, "Automatic segmentation of the liver for preoperative planning of resections," *Stud. Health Technol. Inform.*, vol. 94, pp. 171–173, 2003.
[17] Y. Boykov and V. Kolmogorov, "Computing geodesics and minimal surfaces via graph-cuts," in *Proc. 4th Int. Conf. Comput. Vision*, Nice, 2003, pp. 26–33.
[18] L. Massoptier and S. Casciaro, "Advanced image processing techniques for liver tissue classification," in *New Technology Frontiers in Minimally Invasive Therapies*. Lecce, Italy: Lupiensis Biomedical Publications, 2007, pp. 35–42.
[19] D. Comaniciu and P. Meer, "Mean shift: A robust approach toward feature space analysis," *IEEE Trans. Pattern Anal. Mach. Intell.*, vol.24, pp. 603–619, May 2002.
[20] J. E. Bartlett, J. W. Kotrlik, and C. C. Higgins, "Organizational research: Determining appropriate sample size in survey research," *Info. Technol. Learn. Perf. J.*, vol. 19, pp. 43–50, Aug. 2001.
[21] L. Massoptier and S. Casciaro, "A new fully automatic and robust algorithm for fast segmentation of liver tissue and tumors from CT scans," *Eur. Radiol.*, vol. 18, pp. 1658–1665, Aug. 2008.
[22] S. J. Lim, Y. Y. Jeong, and Y. S. Ho, "Segmentation of the liver using the deformable contour method on CT images," *LNCS*, vol. 3767, pp.570–581, 2005.
[23] J. Missbach-Guentner, C. Dullin, S. Kimmina, M. Zientkowska, M. Domeyer-Missbach, C. Malz, E. Grabbe, W. Stühmer, and F. Alves,"Morphologic changes of mammary carcinomas in mice over time as monitored by flat-panel detector volume computed tomography," *Neoplasia*, vol. 10, pp. 663–673, 2008.
[24] M. B. Dillencourt, H. Samet, and M. Tamminen, "A general approach to connected-component labeling for arbitrary image representations," *J. Assoc. Comput. Machinery*, vol. 39, pp. 253–280, Apr. 1992.
[25] L. Hermoye, I. Laamari-Azjal, Z. Cao, L. Annet, J. Lerut, B. M. Dawant, and B. E. Van Beers, "Liver segmentation in living liver transplant donors: Comparison of semiautomatic and manual methods," *Radiology*, vol. 234, pp. 171–178, Nov. 2005.
[26] P. A. Yushkevich, J. Piven, H. C. Hazlett, R. G. Smith, S. Ho, J. C. Gee, and G. Gerig, "User-guided 3D active contour segmentation of anatomical structures: Significantly improved efficiency and reliability," *Neuroimage*, vol. 31, pp. 1116–1128, Jul. 2006.
[27] C. Xu and J. L. Prince, "Snakes, shapes, and gradient vector flow," *IEEE Trans. Image Process.*, vol. 7, pp. 359–369, 1998.
[28] M. Cvancarova, F. Albregtsen, K. Brabrand, and E. Samset, "Segmentation of ultrasound images of liver tumors applying snake algorithms and GVF," in *Proc. Conf. Rec. Int. Congr. Ser. CARS*, 2005, pp. 218–223.
[29] F. Liu, B. Zhao, P. K. Kijewski, L. Wang, and L. H. Schwartz, "Liver segmentation for CT images using GVF snake," *Med. Phys.*, vol. 32, pp. 3699–3706, Nov. 2005.

ISSN: 2278 – 1323